Sutthaweekul R, Tian GY.

Steel Corrosion Stages Characterisation using Open-Ended Rectangular Waveguide Probe.

***IEEE Sensors Journal* (2017)**

DOI: https://doi.org/10.1109/JSEN.2017.2775521

Steel Corrosion Stages Characterisation using Open-Ended Rectangular Waveguide Probe

Ruslee Sutthaweekul, *Student Member, IEEE* and Gui Y. Tian, *Senior Member, IEEE*

***Abstract*— Safety evaluation of steel structures requires knowledge of corrosion progression stages. The deteriorative stage of corrosion involves multiple parameters, and thus it is difficult to be characterised by model-based approaches. In this work, we propose a steel corrosion stages characterisation method using microwave open-ended rectangular waveguide (ORWG) probes and a statistical-based principal component analysis (PCA) method. Two ORWG probes operating in successive bands, ranging between 9.5 to 26.5 GHz, are utilised to obtain reflection coefficient spectra from specific sets of corrosion samples; i.e., uncoated corrosion progression, coated corrosion progression and surface preparation. PCA is applied to extract corrosion progression feature from spectral responses of training samples. The robustness of the PC-based features is analysed with influences of operating frequency, coating layer and surface condition. It is found that the corrosion feature extracted by the first principal component (PC1) from coated and uncoated corrosion samples are highly correlated to the corrosion progress regardless of probe parameter and coating layer.**

***Index Terms*— Corrosion characterisation; Open-ended rectangular waveguide probe; Principal component analysis; Corrosion progression feature.**

I. Introduction

STEEL is known as the most common material for building and engineering equipment. It provides strength to the structures, however, deteriorated overtime by corrosion when exposed to environments, in particular, polluted or marine atmospheric areas. Corrosion cost money and lives, together with other indirect costs, thus characterisation of corrosion progression stages is crucial for maintenance and structural safety evaluation. Corrosion may also occur under the coating layers (e.g., primer, paint, or insulation), which is difficult to be detected by simple visual inspection. Therefore, various non-destructive testing (NDT) methods [1], [2] have been attempted to characterise hidden corrosion or corrosion undercoating. For instance, fibre Bragg grating (FGB) [3] and acoustic emission (AE) methods [4] are sensitive to volumetric changes but require installation of equipment with extended period of data acquisition. An electrical impedance method such as electrochemical impedance spectroscopy (EIS) [5] can quickly measure the capacitance of coating and corrosion but requires complex data analysis for quantification and it is not suitable for in-situ inspection. Low frequency electromagnetic (EM) methods such as pulsed eddy current (PEC) [6] and low-frequency radio-frequency identification (LF-RFID) sensors [7] are more sensitive to presences of metal loss, which only occur in the late corrosion progress. In the initial corrosion progress (before the presence of metal loss or substrate dissolution), the success of corrosion stages characterisation significantly depends on the sensitivity of sensors and their features that can distinguish among tiny changes of corrosion properties as well as corrosion thickness. Microwave and millimetre wave methods are attractive for corrosion stages characterisation regarding good penetration and sensitive to changes in dielectric layers including iron oxide [8], [9]. Moreover, the study of Kim et al. [10] found that the spectral response of early-stage corrosion has characteristic shapes that can be useful for corrosion characterisation in GHz range. Among microwave sensors, open-ended waveguides are the most suitable probes for near-field inspection having merits of small aperture, well-confined wave propagation with orientation dependence (rectangular probe) and wideband. The open-ended waveguide probes have demonstrated a capability for inspection of layered and composite structures [11], [12].

In previous corrosion studies using open-ended rectangular waveguide (ORWG) probes with model-based approaches, corrosion on aluminium and steel substrates have been modelled as a thin dielectric layer backed by a perfect conductor plate [13], [14]. The study of steel corrosion under paint by Qaddoumi et al. [14] utilised an ORWG probe to obtain the phase of reflection coefficients over the coated corrosion samples with the help of a reflectometer. Thicknesses of coating and corrosion layers were determined from phase responses at a specific frequency. As the development of multilayer inverse model, Ghasr et al. [14] introduced a full-wave accurate model and iterative inverse technique for estimating the complex permittivity and thicknesses of dielectric layers. It has shown good accuracy in thickness evaluation of lined-fibreglass [12] and the coating layer of carbon fibre composites [15]. Although more and more researchers have unveiled the layer properties with the improvement of measurement techniques, it is still difficult to estimate the steel corrosion progress from its

The authors would like to thank EPSRC and EU for funding the work, thank International Paint Ltd for providing the dedicated samples and thank Trevor Wills from the International Paint Ltd for useful suggestions.

The authors are with the School of Electrical and Electronic Engineering (EEE), Newcastle University, United Kingdom, NE1 7RU (email: {r.sutthaweekul1 and g.y.tian}@newcastle.ac.uk).

This article has been accepted for publication in a future issue of this journal, but has not been fully edited. Content may change prior to final publication. Citation information: DOI 10.1109/JSEN.2017.2775521, IEEE Sensors Journal

properties since the thickness and chemical compound are varying over time [10], [16], [17]. So far, there is no comprehensive study of open-ended waveguide measurement related to corrosion progression and complex changes in the corrosion layer properties.

In contrast to the model-based approaches, the statistical-based approach such as principal component analysis (PCA) relies on sampling data obtained from a correlated set of training samples. PCA determines the major factors (a set of linearly uncorrelated weighted vectors) from a multidimensional and multivariate dataset. Unlike the model-based regression, PCA may not be able to quantify individual physical parameters if those parameters contribute to the same kind of response (e.g., increasing of thickness and tangent loss in material both will decrease magnitude response). However, it has potential to characterise multivariate parameter such as corrosion progress with a high chance of elimination the irrelevant influences. PCA has been successfully applied to analyse spectra of complex chemical and physical dielectric bodies. For instance, Regier et al. [18] proposed a measurement technique based on dielectric spectroscopy combined with PCA to analyse both particle size and volume fraction of nutrition. Sophian et al. [19] used PCA for feature extraction of PEC responses of metal defects. The tests carried out show superior defect classification performance over the conventional method. The recent study using an ORWG probe in cooperation with PCA for inspection of protective linings (organic coating), so-called the chemometric method, was carried out by Miszczyk et al. [20]. This technique is based on feature extraction of magnitude spectra varied by electromagnetic wave absorbing properties of the defect linings. Without an analytical model and prior knowledge of lining's properties, the results indicate that the lining defects such as presences of wet or dry corrosion and air-gap can be characterised effectively by the first two principal components with the elimination of random interferences. Nevertheless, the corrosion samples used in the study were imitated by corrosion powder, and there was no discussion about the progression stage or related properties of the corrosion samples.

In this paper, we investigate a steel corrosion stages characterisation method using reflection coefficient spectra obtained by ORWG probes and PCA as the feature extraction method. The spectra from three sets of dedicated corrosion progression and surface roughness samples are obtained by means of VNA with two probes. We apply PCA to extract corrosion progression features from the obtained spectra of each probe. The robustness of the extracted features is analysed by projected with the sampling data of each sample. The rest of this paper are organised as follows. Section II describes the operational principle of open-ended waveguide probe, an illustration of corrosion undercoating, and the preparation of three corrosion sample sets. Section III demonstrates the experimental setup, measurement procedures and data analysis using PCA. The quantitative analysis of the measurement results is presented and discussed in Section IV. Finally, Section V concludes the major findings and the future works.

TABLE I
THE PROPERTIES OF WR-62 AND WR-42 PROBES IN TE_{10} MODE

Probe no.	Dimensions a x b (mm)	Normal operating frequencies (GHz)	Cut-off frequency (GHz)
WR-62	15.80 x 7.90	12.4 – 18.0	9.5
WR-42	10.67 x 4.32	18.0 – 26.5	14.1

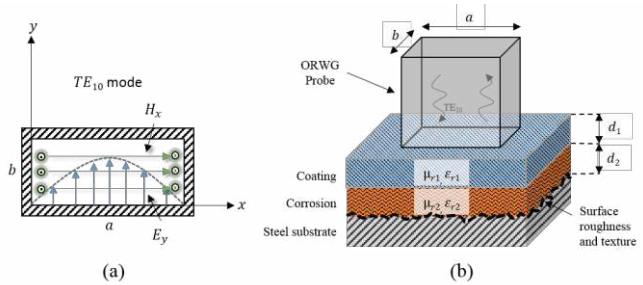

Fig. 1. (a) ORWG probe's aperture and field distribution in TE10 mode and (b) a model of corrosion undercoating inspected by an ORWG probe.

II. MICROWAVE ORWG PROBE MEASUREMENT OF CORROSION UNDERCOATING

In this section, we explain measurement mechanism of an ORWG probe operating in TE_{10} mode, followed by the relationship between reflection coefficient and related parameters of corrosion undercoating and the preparation process of the samples.

A. ORWG Probe Measurement Mechanism

Due to the symmetry of the incident field and the measurement geometry, only rectangular waveguide modes with m = odd (1, 3, 5, …) and n = even (0, 2, 4, …) can be excited at the probe aperture [21]. The calculation of cut-off frequencies at different modes of a waveguide probe are given by

$$fc_{mn} = \frac{1}{2\pi\sqrt{\mu\,\varepsilon}}\sqrt{\left(\frac{m\pi}{a}\right)^2 + \left(\frac{n\pi}{b}\right)^2}, \quad a > b \tag{1}$$

where μ and ε are permeability and permittivity of waveguide filling material, a and b are inner length and width of the waveguide aperture, m and n are integers used to determine the waveguide propagation modes. Based on the frequency responses of the corrosion [10], two sizes of ORWG probes: WR-62 and WR-42 operating in a frequency range between 9.5 – 26.5 GHz, have been chosen in our experiment. The properties of WR-62 and WR-42 probes are shown in Table I.

In this work, we excite the ORWG probes in the dominant TE_{10} mode. Although it is known that the higher order modes are produced by the interrogation between waveguide aperture and samples, this effect is considered insignificant since it affects measurement result for only less than 3% [22]. The ORWG probe has directional E-field property illustrated in Fig.1(a) as the TE_{10} mode aperture field is given by

$$E_y(x,y,0) = \bar{e}_o(x,y) = \begin{cases} \sqrt{\frac{2}{ab}}\cos\left(\frac{\pi x}{a}\right), (x,y) \in aperture \\ 0, (x,y) \notin aperture \end{cases} \tag{2}$$

I, we do not directly measure the electric or magnetic fields but the reflection coefficient (S_{11} or Γ), which relates to a

This article has been accepted for publication in a future issue of this journal, but has not been fully edited. Content may change prior to final publication. Citation information: DOI 10.1109/JSEN.2017.2775521, IEEE Sensors Journal

coupling between the termination impedance of OWRG probe Z_{WG} and impedance at interface of the testing sample Z_{in} as $\Gamma = (Z_{in} - Z_{WG})/(Z_{in} + Z_{WG})$.

The model of corrosion undercoating is considered as two dielectric layers backed by the metallic substrate as illustrated in Fig. 1(b). The interaction between the layered structure and incident waves occurs in the near field of the probe where the electrometric field responses are rather complex. In general, the reflection coefficient is a function of probe dimensions a and b, operating frequency f, relative permittivity ε_{r1} and ε_{r2}, relative permeability μ_{r1} and μ_{r2}, and layer thicknesses $d1$ and $d2$. As mentioned in the previous section, many investigators have methodically worked towards developing full-wave models to describe the complex interaction of nearfields of a waveguide probe with layered structures. In contrast to the model-based inversion, this work is based on experimental studies of spectral responses obtained from corrosion progression samples. A statistical-based PCA method is not intended to determine actual parameters such as corrosion thickness and its material properties but is applied for feature extraction of a multivariate parameter such as corrosion progress. It is expected that the selected PCA based features can be used for quantitative non-destructive evaluation (QNDE) of the corrosion progression stages regardless of model analysing and parameters estimation. Three sets of dedicated samples are used for PCA training and testing robustness of selected PC-based features.

B. Samples and Preparation

To study corrosion progress together with the influences of the coating layer and surface condition, we selected three dedicated sets of samples. The samples have been prepared as follows.

1) Uncoated Corrosion Progression Samples (UP)

Shown in Fig.2(a), these samples were prepared as follows: firstly, a plate of un-corroded mild steel (S275) was cut into pieces of 300 mm x 150 mm x 3 mm (length x width x thickness). After cutting, we covered the whole plates with plastic tape excluding the central area of 30 mm x 30 mm to let corrosion develop. Finally, they were exposed to the marine atmosphere at different periods of 1, 3, 6, 10, and 12 months (UP1, UP3, UP6, UP10, and UP12). It is noted that the sample UP0 used in this study is a measurement of the un-corroded area of the UP1 sample.

TABLE III
MEASUREMENT PARAMETERS

Parameter	Value
Type of Samples	UP – uncoated corrosion progression CP – coated corrosion progression US – uncoated surface preparation
Probe No. / Sweeping frequency ranges	WR-62 / • 12.0 -18.0 GHz (UP and US) • 9.5 - 18.0 GHz (CP) WR-42 / • 18.0 - 26.5 GHz
Sampling frequency points	1601
Probe orientation	0° and 90°

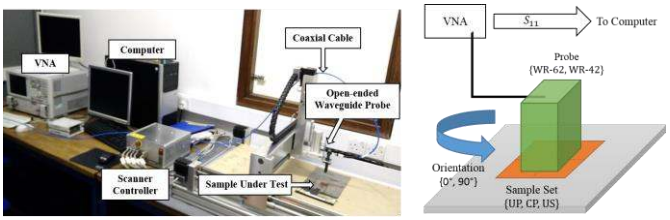

Fig. 3. Equipment setup and experiment for obtaining reflection coefficients over corrosion samples

2) Coated Corrosion Progression Samples (CP)

Initially, these samples were prepared using the same process as of the UP samples. They were coated by non-conductive (dielectric) paint with the average thickness of approximately 100 µm resulting in products of coated corrosion progression samples (CP1-CP12) as shown Fig. 2(b). It is noted that the sample CP0 is a measurement of coating area without corrosion of the CP1 sample.

3) Uncoated Surface Preparation Samples (US)

Shown in Fig. 2(c), the samples were prepared as follows: initially, three out of four steel plates (US2-US4), sizing of 300 mm x 100 mm, were placed in an environmental test chamber for a month to accelerate the corrosion progress over the samples. Following this, the surface of each sample has been treated differently according to Steel Structures Painting Council (SSPC) standard [23]. The final products

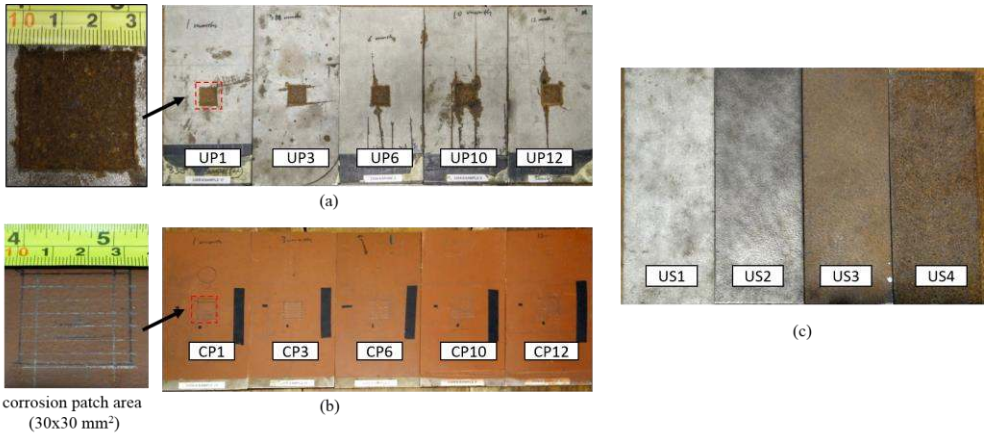

Fig. 2. Corrosion sample sets: (a) uncoated corrosion progression (UP), (b) coated corrosion progression (CP), and (c) uncoated surface preparation (US).

of samples with different surface roughness, with and without presences of corrosion are described in Table II.

III. Experimental Studies and Feature Extraction using PCA

Equipment setup of microwave ORWG system for corrosion stages characterisation is shown in Fig. 3. The hardware system is composed of an X-Y-Z scanner (High-Z S-720), a vector network analyser (VNA, Agilent PNA E8363B) and a computer connected to the VNA through a general propose interface bus (GPIB) and through to the scanner via a parallel port interface. We programmed the scanner to deploy the waveguide probe positioning over the testing samples. Before the measurement, we calibrate the VNA together with the coaxial cable using a calibration kit (open, short and load). The calibration results are used to compensate the cable characteristic and delay of the channel.

Three experiments with three sets of samples are conducted in this study as described in Table III. For each set of samples, reflection coefficients are sampled ten times at slightly different positions (about 0.2 mm) of the corrosion patch centre with 0° and 90° orientations using WR-62 and WR-42 probes. Amount of measurements performed for each set calculated by a number of samples in each set × probes × orientations are 240, 240 and 160 for samples UP, CP and US, respectively. In these sampling data, seven out of ten are used for PCA training; while the rest are used to test selected principal components. It is noted that the operating frequency of WR-62 probe of CP samples is extended to the cut-off frequency at 9.5 GHz to capture the shifted frequency responses caused by the coating material. It is known that the operating frequency closing to the cut-off is not recommended, as it is highly dispersive due to steep change of phase velocity or group delay. However, the quantities analysed in this work are only the magnitude response $|S_{11}|$, which is independent to phase variation and thus robust to dispersion. Moreover, unlike pulsed radars, the operation of VNA will transmit single frequency or very narrow band FMCW signals at a time in a sweeping manner. Therefore, the obtained magnitude responses from VNA are unlikely to suffer by the effect of wave dispersion.

To extract corrosion progression parameter from the training data, PCA method is applied to decompose principal components. The process of PCA shown in Fig. 4 includes two major steps: training and testing. In training step, we form covariance matrices of sampling data of each sample sets categorised by the measurement probe and then calculate roots of eigenvectors e_i and corresponding eigenvalues λ_i using Eigenvector decomposition. The eigenvectors sorted by descending order of eigenvalues are called principal components (PCs). According to the cumulative percentage of variances $(\lambda_i/\sum_{i=1}^{n}\lambda_i)$, we usually choose only a few most contributed k principal components to test for the major contributed parameter. In the testing step, the sampling data from testing dataset are projected to the k chosen PCs. The projected value, which is a linear combination between PC coefficients and sampling data, represents a PC feature. One of the major PCs having its projected values most correlated among corrosion datasets will be chosen for feature extraction of the corrosion progression. Besides, the influences of inhomogeneity in material and surface conditions are also studied through comparison of PC features at 0° and 90°.

IV. Results and Discussion

In this section, reflection coefficient spectra obtained from three sample sets are presented. We choose three most contributed principal component PC1-PC3 to test for feature extraction of corrosion progression. The projected values of PC1-PC3 to testing data are analysed. Finally, we discuss other measurement influences such as probe orientation and surface condition.

A. Reflection Coefficient Responses of Corrosion Progression Samples

The magnitude responses obtained from 7 slightly different sampling positions of UP and CP samples with different probes and orientations are shown in Fig. 5 and Fig.6. It can be seen that the spectra of the WR-62 probe, Fig. 5(a)-(f) and Fig. 6(a)-(f), show single resonant responses while that of the WR-42 probe, Fig.5(g)-(l) and Fig.6(g)-(l), show multiple resonances and ripples. Also, the variations of response in the resonant region are significantly higher than the flat response region. The differences in the responses of two probes are caused by the interaction between signal coherence, thickness and material properties at different probe dimensions and operating frequencies. Moreover, the unwanted ripples could be generated by the interrogation between the sample and the edge of unmodified finite flange probe [24]. Besides, it is found in general that the influence of probe orientation is very little in the beginning progress up to 6 months and becomes more significant in the 10 and 12 months.

To study the influences of the coating layer only, we obtained reflection coefficients from the CP samples in the area outside corrosion patch. The sampling data are labelled as C1-C12 according to the CP1-CP12 samples. Although these samples have been painted with the same coating material, the thicknesses of coating layer in each sample may be varying due to the manufacturing uncertainty. From the responses of the WR-62 probe shown in the Fig. 7(a), we find that the resonant frequency of all sampling data is consistent at around 10.5 GHz demonstrating highly dependent on the coating material, whilst resonant magnitudes are varied by coating thicknesses. On the other hand, the responses of the WR-42 probe in higher frequency shown in Fig. 7(b) demonstrate complex responses of multiple resonances similarly to that of the CP samples.

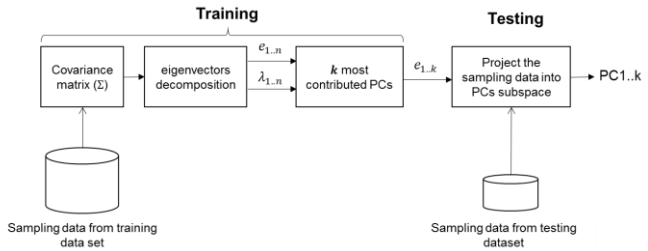

Fig. 4. PCA for feature extraction of corrosion progression.

This article has been accepted for publication in a future issue of this journal, but has not been fully edited. Content may change prior to final publication. Citation information: DOI 10.1109/JSEN.2017.2775521, IEEE Sensors Journal

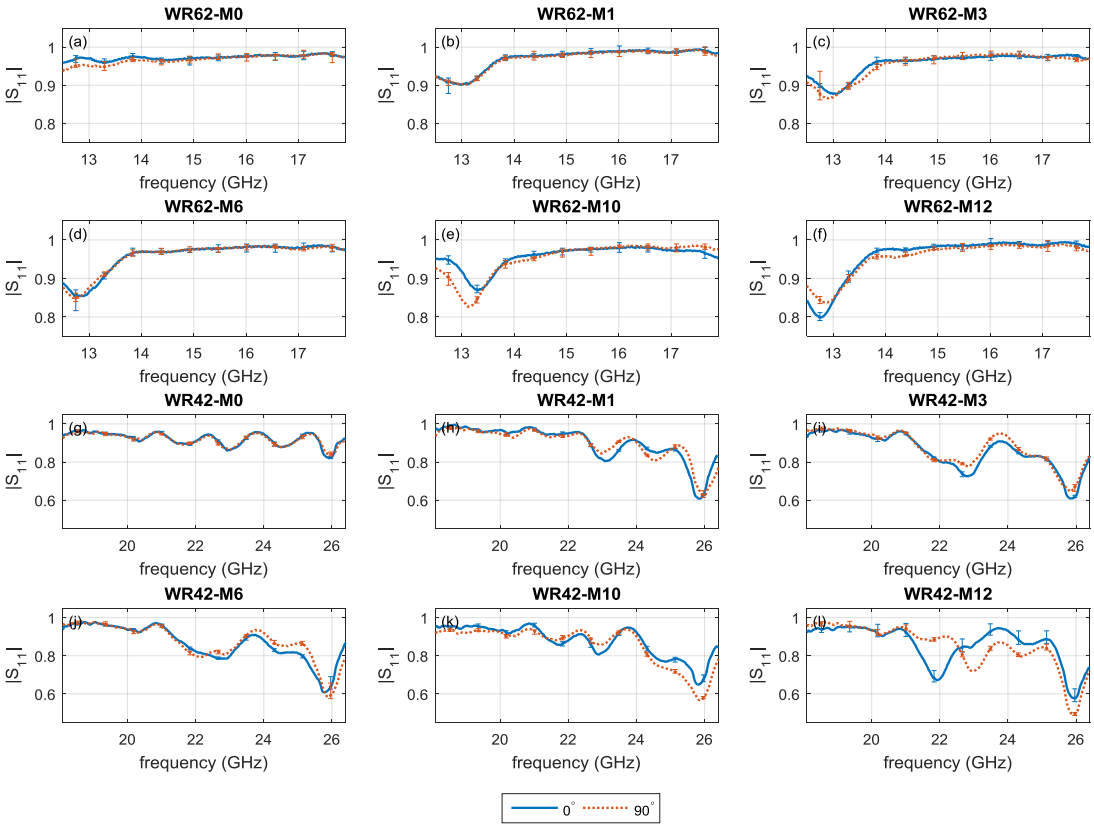

Fig. 5. Average magnitude responses of UP samples obtained by WR-62: (a) M0, (b) M1, (c) M3, (d) M6, (e) M10, (f) M12 and WR-42: (g) M0, (h) M1, (i) M3, (j) M6, (k) M10, (l) M12.

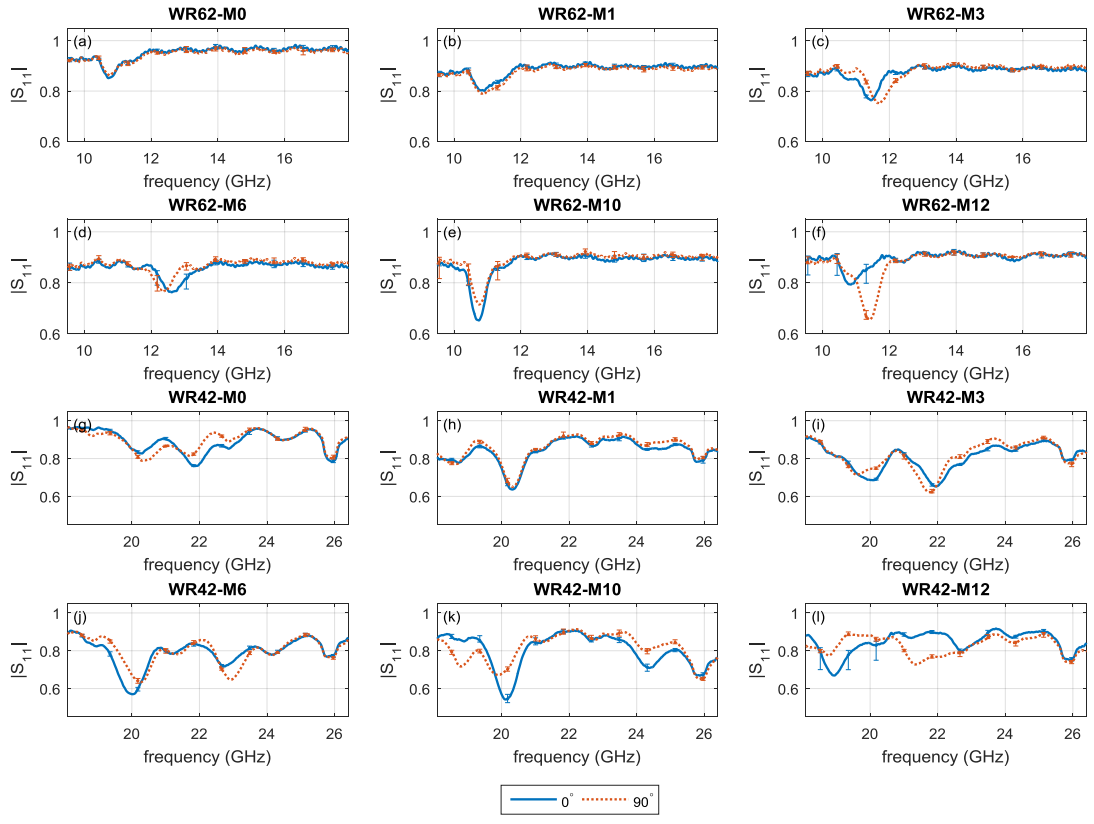

Fig. 6. Average magnitude responses of CP samples obtained by WR-62: (a) M0, (b) M1, (c) M3, (d) M6, (e) M10, (f) M12 and WR-42: (g) M0, (h) M1, (i) M3, (j) M6, (k) M10, (l) M12.

This article has been accepted for publication in a future issue of this journal, but has not been fully edited. Content may change prior to final publication. Citation information: DOI 10.1109/JSEN.2017.2775521, IEEE Sensors Journal

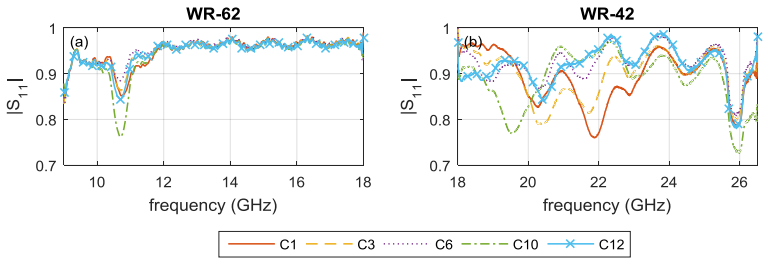

Fig. 7. Average magnitude of the reflection coefficients of the coating layer from CP samples (C1-C12) measured by (a) WR-62 and (b) WR-42.

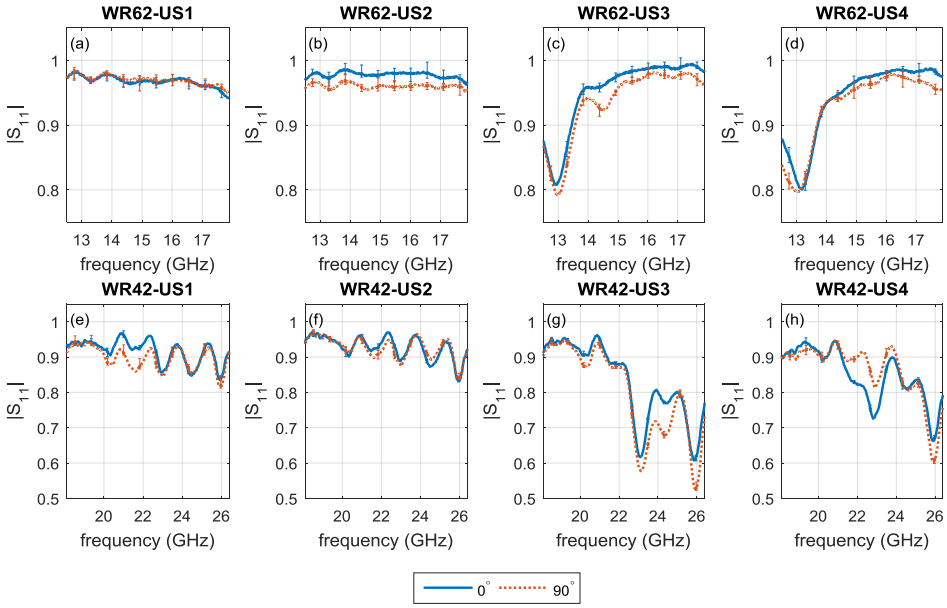

Fig. 8. Average magnitude responses of US samples obtained by WR-62: (a) US1, (b) US2, (c) US3, (d) US4 and WR-42: (e) US1, (f) US2, (g) US3, (h) US4.

In the study of surface influence of US samples, the responses of WR-62 probe plotted in Fig. 8(a)-(d) show no significant variation at different orientations. However, the samples US3 and US4, which are the samples with presences of corrosion, demonstrate strong resonant response similar to that of the UP samples. Fig. 8(e)-(h) show responses of US samples measured by WR-42 probe. Moreover, the influence of orientation is only recognisable in the samples US3 and US4 which are corroded samples.

Nevertheless, it is difficult to analyse the complex responses of spectral feature (1601 frequency components) and identify distinguish parameters. Hence, PCA is applied to extract major principal components from the training responses. It is expected that one of obtained principal components can be used to extract a feature that represents corrosion progression.

B. PCA for Feature Extraction of Corrosion Progression

We apply PCA to extract and analyse the major contributed parameters from high-dimensional features (1601 sampling frequency points). The summations of the percentage of variance of the first three principal components of each dataset are higher than 90%, therefore in our study, only PC1-3 are selected for feature extraction. The high percentage of variance of the first three PCs also indicates that the sampling data in each dataset are greatly correlated and should be sufficient to extract the major contributed parameter. To identify the corrosion progression features from the selected PCs, we project 3 sampling data from test dataset to the selected PC1-3 vectors of their own set. The projected values of PC1-3 are plotted in Fig.9; the standard deviations of projected values based on 6 sampling data in each progression (3 sampling by 2 orientations) are shown in Table IV. Concerning orientation, we find that the deviation of PC1-3 features between 0 to 6 months are insignificant. Whilst the variations are stronger in 10 and 12 months, specifically, the UP samples. The results may be explained by the fact that corrosion at the surface of UP10 and UP12 have been severe flaked-off. Thus, it introduces random roughness and inhomogeneity in these samples.

The deviation of PC1-3 features extracted from three test samples are shown by min/max lines in Fig. 9. It is found, in general, that deviations are quite noticeable in particular the PC1 features. The discrepancy could be attributed to higher variation in the resonant region representing corrosion responses. Moreover, it is obvious that the deviation of PC2 and PC3 features in Fig. 9(b) and (c) are relatively strong. It is due to the high correlation and least complex responses of UP samples obtained by WR-62 probes demonstrated in Fig. 5(a)-(f). Hence, PC1 mainly contributes to the percentage of variance while the lower PCs could be regarded as the noise sub spaces.

This article has been accepted for publication in a future issue of this journal, but has not been fully edited. Content may change prior to final publication. Citation information: DOI 10.1109/JSEN.2017.2775521, IEEE Sensors Journal

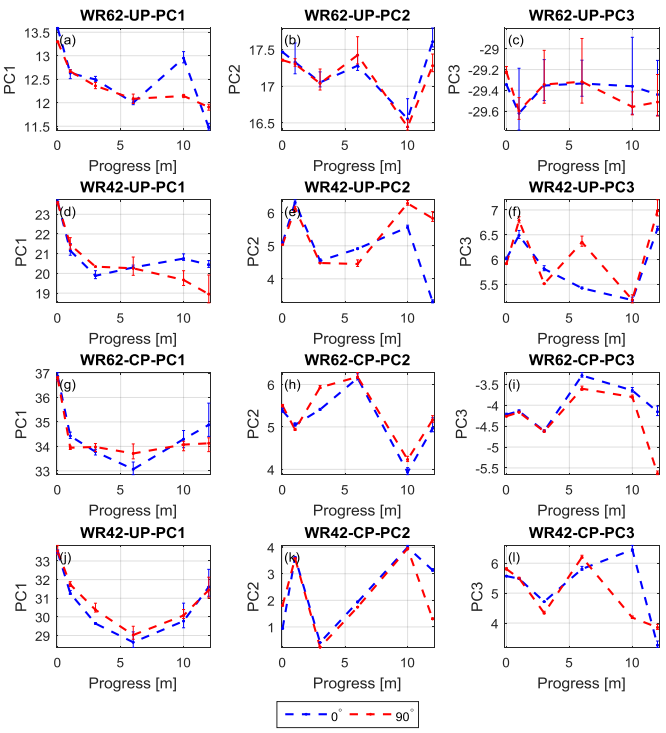

Fig. 9. PC1-PC3 projected values of UP samples: (a) WR-62 PC1, (b) WR-62 PC2, (c) WR-62 PC3, (d) WR-42 PC1, (e) WR-42 PC2, (f) WR-42 PC3; PC projected values of CP samples: (g) WR-62 PC1, (h) WR-62 PC2, (i) WR-62 PC3, (j) WR-42 PC1, (k) WR-42 PC2 and (l) WR-42 PC3.

TABLE IV
STANDARD DEVIATIONS OF UNCOATED (UP) AND COATED (CP) CORROSION SAMPLES AT 0° AND 90°

	PC	Probe No.	M0	M1	M2	M6	M10	M12
UP	PC1	WR-62	0.16	0.07	0.09	0.09	0.45	0.25
		WR-42	0.05	0.24	0.27	0.20	0.62	0.88
	PC2	WR-62	0.06	0.09	0.08	0.12	0.11	0.20
		WR-42	0.03	0.11	0.04	0.26	0.40	1.38
	PC3	WR-62	0.07	0.16	0.13	0.15	0.19	0.14
		WR-42	0.06	0.17	0.16	0.51	0.04	0.21
CP	PC1	WR-62	0.13	0.28	0.17	0.45	0.29	0.67
		WR-42	0.11	0.27	0.42	0.31	0.39	0.39
	PC2	WR-62	0.07	0.06	0.29	0.05	0.17	0.14
		WR-42	0.47	0.02	0.10	0.11	0.04	1.00
	PC3	WR-62	0.03	0.02	0.02	0.18	0.09	0.81
		WR-42	0.13	0.02	0.21	0.22	1.24	0.33

Interestingly, the plots of PC1 projected values against corrosion progress of UP and CP samples of both probes demonstrated in Fig. 9(a), (d), (g) and (j), render highly correlated curves that could represent the common parameter, which is corrosion progress. The agreement between PC1 projected values indicates that the PC1 features are independent of the probe and coating parameters (i.e., operating frequency f, probe dimensions a/b, coating thickness and properties). Moreover, we find that the characteristic of the PC1 features is in line with the previous corrosion study using ultra high frequency (UHF) RFID and PCA of the same samples [25].

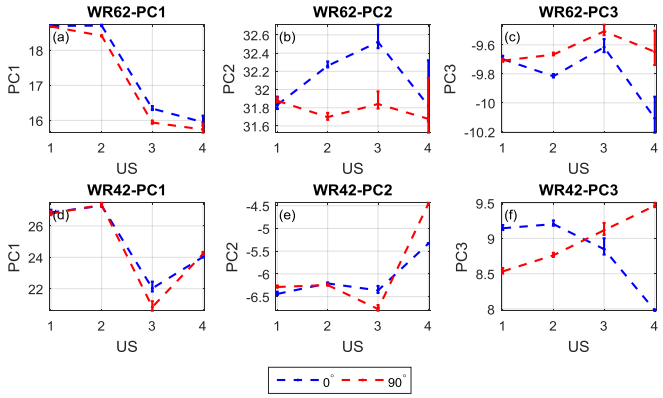

Fig. 10. PC1-PC3 projected values of US samples: (a) WR-62 PC1, (b) WR-62 PC2, (c) WR-62 PC3, (d) WR-42 PC1, (e) WR-62 PC2, (f) WR-62 PC3.

TABLE V
STANDARD DEVIATIONS OF UNCOATED SURFACE PREPARATION (US) SAMPLES AT 0° AND 90°

	PC	Probe No.	US1	US2	US3	US4
US	PC1	WR-62	0.02	0.16	0.22	0.18
		WR-42	0.09	0.08	0.68	0.11
	PC2	WR-62	0.04	0.31	0.38	0.26
		WR-42	0.09	0.02	0.23	0.48
	PC3	WR-62	0.01	0.08	0.06	0.26
		WR-42	0.34	0.24	0.16	0.81

In the low frequency electromagnetic method such as PEC [6], a corrosion progression feature has been found corresponding to corrosion thickness and metal loss affecting the average conductivity and permeability. Although the corrosion feature of PEC demonstrates a monotonic relationship to the corrosion progress, its sensitivity is low due to the influence of conductive substrate. In contrast, microwave is sensitive to changes in dielectric properties caused by the chemical process [10], [26]. The measurement results are related to the impedance matching between probe's aperture and the dielectric layers including coating and corrosion layers with little influence of the conductive substrates (microwaves are totally reflected at the metallic interface). Nonetheless, microwave signals are more sensitive to the structural influences such as material inhomogeneity or surface roughness [27], [28] , hence an advanced data analysis method is required for feature extraction.

For US samples, the plots of PC1-3 projected values and the corresponding standard deviations are shown in Fig. 10 and Table V. It is obvious in the results that the PC1 represents corrosion feature as demonstrated by distinguishable values between US1/US2 and US3/US4. However, influence of orientation is insignificant in PC1 but can be noticeable in PC2 and PC3 features. It is worth to continue investigation in the future work with more dedicated surface samples (e.g., surface roughness and manufacturing process with different directional texture).

V. CONCLUSIONS

We study two microwave open-ended rectangular waveguide probes with coated/uncoated corrosion progression and surface preparation samples for corrosion stages characterisation. The

responses of obtained reflection coefficients are analysed for corrosion progression feature using PCA. Unlike the model-based regression methods, our proposed method is not intended and is not capable of actual corrosion parameter estimation such as thickness and complex dielectric properties of corrosion. The PC-based feature is only used as an indicator for changes of the corrosion progression stages. The major findings in our work are summarised as follows.

1. The microwave inspection method using open-ended waveguide probe and PCA is a promising tool for steel corrosion stages characterisation. The interaction between ORWG probe and corrosion layer is highly sensitive as resulting in variation of resonant responses. PCA is applied to extract the corrosion progression feature from the responses. It is found that the PC1 features are independent of probe and coating parameters and can be used to characterise corrosion progression stages.
2. Based on the investigation of ORWG probes at different operating frequencies, it is found that the responses from WR-62 probe operating at a frequency range between 9.5 GHz – 18 GHz are steadier for both coated and uncoated corrosion. The WR-42 probe, on the other hand, gives multiple resonances and is sensitive to other influences such as surface roughness as indicated in the PC3 features of the US samples.
3. As indicated in Fig. 9(a), (d), (g) and (j), we found a turning point at around 6 months of the PC1 features. The initial falling trend is likely to be related to the increasing of corrosion thickness in early corrosion stages. Whereas the influence of material properties becomes stronger and causes reverse inclination in the latter stages.

Future work, we will involve a comparison between the corrosion progression feature extracted using PCA and the model-based parameters related to corrosion progress (i.e., corrosion properties and thickness). Other advanced feature extraction techniques will be studied to overcome the non-linear characteristic of the corrosion feature.

REFERENCES

[1] X. Qi and V. J. Gelling, "A Review of Different Sensors Applied to Corrosion Detection and Monitoring," *Recent Pat. Corros. Sci.*, vol. 1, no. 1, pp. 1–7, Jun. 2011.

[2] A. Zaki, H. K. Chai, D. G. Aggelis, and N. Alver, "Non-Destructive Evaluation for Corrosion Monitoring in Concrete: A Review and Capability of Acoustic Emission Technique," *Sensors*, vol. 15, no. 8, pp. 19069–19101, Aug. 2015.

[3] S. K. T. Grattan, S. E. Taylor, T. Sun, P. A. M. Basheer, and K. T. V. Grattan, "Monitoring of Corrosion in Structural Reinforcing Bars: Performance Comparison Using In Situ Fiber-Optic and Electric Wire Strain Gauge Systems," *IEEE Sens. J.*, vol. 9, no. 11, pp. 1494–1502, Nov. 2009.

[4] S. Park, S. Kitsukawa, K. Katoh, S. Yuyama, H. Maruyama, and K. Sekine, "Development of AE Monitoring Method for Corrosion Damage of the Bottom Plate in Oil Storage Tank on the Neutral Sand under Loading," *Mater. Trans.*, vol. 47, no. 4, pp. 1240–1246, 2006.

[5] V. Barranco, S. Feliu Jr., and S. Feliu, "EIS study of the corrosion behaviour of zinc-based coatings on steel in quiescent 3% NaCl solution. Part 1: directly exposed coatings," *Corros. Sci.*, vol. 46, no. 9, pp. 2203–2220, Sep. 2004.

[6] Y. He, G. Tian, H. Zhang, M. Alamin, A. Simm, and P. Jackson, "Steel Corrosion Characterization Using Pulsed Eddy Current Systems," *IEEE Sens. J.*, vol. 12, no. 6, pp. 2113–2120, Jun. 2012.

[7] A. I. Sunny, G. Y. Tian, J. Zhang, and M. Pal, "Low frequency (LF) RFID sensors and selective transient feature extraction for corrosion characterisation," *Sens. Actuators Phys.*, vol. 241, pp. 34–43, Apr. 2016.

[8] H. Luo, R. Gong, X. Wang, Y. Nie, Y. Chen, and V. G. Harris, "Fe3O4 cladding enhanced magnetic natural resonance and microwave absorption properties of Fe0.65Co0.35 alloy flakes," *J. Alloys Compd.*, vol. 646, pp. 345–350, Oct. 2015.

[9] F. Xu, L. Ma, Q. Huo, M. Gan, and J. Tang, "Microwave absorbing properties and structural design of microwave absorbers based on polyaniline and polyaniline/magnetite nanocomposite," *J. Magn. Magn. Mater.*, vol. 374, pp. 311–316, Jan. 2015.

[10] S. Kim, J. Surek, and J. Baker-Jarvis, "Electromagnetic Metrology on Concrete and Corrosion," *J. Res. Natl. Inst. Stand. Technol.*, vol. 116, no. 3, pp. 655–669, 2011.

[11] A. J. Jundi and N. N. Qaddoumi, "Near-field microwave model of multilayered structures illuminated by open-ended rectangular waveguides," *IET Microw. Antennas Propag.*, vol. 6, no. 1, pp. 100–107, Jan. 2012.

[12] M. T. Ghasr, M. J. Horst, M. Lechuga, R. Rapoza, C. J. Renoud, and R. Zoughi, "Accurate One-Sided Microwave Thickness Evaluation of Lined-Fiberglass Composites," *IEEE Trans. Instrum. Meas.*, vol. 64, no. 10, pp. 2802–2812, Oct. 2015.

[13] D. Hughes *et al.*, "Microwave Nondestructive Detection of Corrosion Under Thin Paint and Primer in Aluminum Panels," *Subsurf. Sens. Technol. Appl.*, vol. 2, no. 4, pp. 435–471, Oct. 2001.

[14] N. N. Qaddoumi, W. M. Saleh, and M. Abou-Khousa, "Innovative Near-Field Microwave Nondestructive Testing of Corroded Metallic Structures Utilizing Open-Ended Rectangular Waveguide Probes," *IEEE Trans. Instrum. Meas.*, vol. 56, no. 5, pp. 1961–1966, Oct. 2007.

[15] R. Zoughi, J. R. Gallion, and M. T. Ghasr, "Accurate Microwave Measurement of Coating Thickness on Carbon Composite Substrates," *IEEE Trans. Instrum. Meas.*, vol. 65, no. 4, pp. 951–953, Apr. 2016.

[16] D. de la Fuente, I. Díaz, J. Simancas, B. Chico, and M. Morcillo, "Long-term atmospheric corrosion of mild steel," *Corros. Sci.*, vol. 53, no. 2, pp. 604–617, Feb. 2011.

[17] M. Morcillo, D. De la Fuente, I. Díaz, and H. Cano, "Atmospheric corrosion of mild steel," *Rev. Metal.*, vol. 47, no. 5, pp. 426–444, Oct. 2011.

[18] M. Regier, H. Schubert, and H. P. Schuchmann, "Dielectric spectroscopy-a new method for particle size- and fraction-determination," *Innov. Food Sci. Emerg. Technol.*, vol. 2, no. 5, pp. 199–204, 2004.

[19] A. Sophian, G. Y. Tian, D. Taylor, and J. Rudlin, "A feature extraction technique based on principal component analysis for pulsed Eddy current NDT," *NDT E Int.*, vol. 36, no. 1, pp. 37–41, Jan. 2003.

[20] A. Miszczyk and K. Darowicki, "Inspection of protective linings using microwave spectroscopy combined with chemometric methods," *Corros. Sci.*, vol. 64, pp. 234–242, Nov. 2012.

[21] M. W. Hyde, A. E. Bogle, and M. J. Havrilla, "Nondestructive Characterization of PEC-Backed Materials Using the Combined Measurements of a Rectangular Waveguide and Coaxial Probe," *IEEE Microw. Wirel. Compon. Lett.*, vol. 24, no. 11, pp. 808–810, Nov. 2014.

[22] S. Bakhtiari, S. I. Ganchev, and R. Zoughi, "Open-ended rectangular waveguide for nondestructive thickness measurement and variation detection of lossy dielectric slabs backed by a conducting plate," *IEEE Trans. Instrum. Meas.*, vol. 42, no. 1, pp. 19–24, Feb. 1993.

[23] S. S. P. Council, "Surface preparation," *Syst. Specif.*, vol. 2, 1991.

[24] M. Kempin, M. T. Ghasr, J. T. Case, and R. Zoughi, "Modified Waveguide Flange for Evaluation of Stratified Composites," *IEEE Trans. Instrum. Meas.*, vol. 63, no. 6, pp. 1524–1534, Jun. 2014.

[25] J. Zhang and G. Tian, "UHF RFID Tag Antenna-Based Sensing for Corrosion Detection amp; Characterization Using Principal Component Analysis," *IEEE Trans. Antennas Propag.*, vol. PP, no. 99, pp. 1–1, 2016.

[26] J. A. Cuenca *et al.*, "Study of the magnetite to maghemite transition using microwave permittivity and permeability measurements," *J. Phys. Condens. Matter*, vol. 28, no. 10, p. 106002, 2016.

[27] A. Sentenac, H. Giovannini, and M. Saillard, "Scattering from rough inhomogeneous media: splitting of surface and volume scattering," *J. Opt. Soc. Am. A*, vol. 19, no. 4, p. 727, Apr. 2002.

[28] O. J. F. Martin and M. Paulus, "Influence of metal roughness on the near-field generated by an aperture/apertureless probe," *J. Microsc.*, vol. 205, no. 2, pp. 147–152, Feb. 2002.

Ruslee Sutthaweekul (S'16) received the B.Eng degree in electrical engineering from King Mongkut's University of Technology North Bangkok, Thailand, in 2000, the M.Eng degree in Electrical Engineering and Information Technology from University of Applied Science Rosenheim, Germany, in 2003, and is currently working toward the Ph.D. degree at School of Electrical and Electronic Engineering, Newcastle University, United Kingdom. In 2014, he joined the Communications, Sensors, Signal and Information Processing Research Group, Newcastle University. His research interests include microwave signal processing and imaging, and ground penetrating radar.

Gui Y. Tian (M'01–SM'03) received his B.Sc. degree and M.Sc. degree from University of Sichuan, Chengdu, China in 1985 and 1988, respectively, and Ph.D. from University of Derby, Derby, UK, in 1998. He is currently the Professor of Sensor Technologies at School of Electrical and Electronic Engineering, Newcastle University, United Kingdom. His main interests include Electromagnetic sensors, sensor array and sensor network, Electromagnetic Non-destructive Evaluation, Advanced signal processing and Integrative systems and applications. He has coordinated several research projects from the Engineering and Physical Sciences research Council (EPSRC), Royal Academy of Engineering and FP7. Also he has good collaboration with leading industrial companies such as Airbus, Rolls Royce, BP, nPower, Network Rail and TWI among others.